Worst-Case Robust Beamforming Design for Wireless Powered Multirelay Multiuser Network With a Nonlinear EH Model

Xinghua Jia, Chaozhu Zhang, *Member, IEEE*, and Il-Min Kim, *Senior Member, IEEE*

***Abstract*—This paper studies joint source and relay beamforming for a wireless powered downlink multirelay multiuser network. Considering nonlinear energy harvesting and imperfect channel state information, we aim to minimize the total transmit power at the base station by jointly optimizing the source beamforming and the relay beamforming weights under the energy causality constraints at the relays and the signal-to-noise ratio constraints at the users. The formulated problem is highly nonconvex, and thus, it is difficult to solve. To solve the problem, we first transform it into a worst-case optimization, and then, an iterative algorithm is developed to solve this worst-case optimization. Numerical results show the advantage of the proposed robust scheme.**

***Index Terms*—Non-linear energy harvesting, robust beamforming, two-hop relay networks, wireless powered communications.**

I. Introduction

Radio frequency wireless powered transfer (WPT) has been a promising technology in wireless communications because it can effectively and stably prolong the lifetime of low-power and energy limited devices [1], [2]. Currently, there are many potential application scenarios being explored combining wireless information and power transfer: e.g., internet of things (IoT) networks and wireless sensors networks [3]. The future wireless sensors or IoT networks will contain billions of devices. Replacing or charging batteries of devices may be very costly and even dangerous in some hazardous environments. By powering the sensors with dedicated energy sources, replacing or manual charging batteries is no longer needed. In addition, without power cable limits, the sensors and devices can be deployed more flexibly and can even be embedded into the walls of buildings.

WPT has also been applied to the cooperative multirelay networks to improve the overall performance of wireless networks and balance the fairness of resource usages [4]–[6]. Considering the existing challenges, the joint resource allocation is an essential issue for multirelay networks to enhance the spectrum and energy efficiencies: e.g., the joint relay selection design [4], the joint power splitting design [5], and the joint beamforming design [6]. Joint beamforming design is one of the key techniques to ensure the energy-efficient communications of wireless powered networks; see [6]–[9] and the references therein. It has been commonly pointed out that the joint beamforming optimization can significantly improve the system performance compared to any fixed schemes. However, all the works above considered the *perfect* channel state information (CSI) and the *ideal* energy-harvesting (EH) model, i.e., constant energy conversion efficiency over infinitely wide input lower range.

In practice, acquiring perfect CSI might be very costly, and thus, it is reasonable to consider the imperfect CSI. In addition, the real EH circuits at the receivers are nonlinear: the practical EH circuitry suffers from the kick-off voltage and the saturation effect [10], [11]. In the literature of non-linear EH models, the non-linear EH model proposed in [12] can accurately match the practical measures results, and thus, has been commonly used in many EH-related works [2], [11], [13]. Also, it has been commonly shown that the system performance achieved with the non-linear EH model is very different from that the system performance achieved with the linear EH model. To the best of our knowledge, there have been no such works in the literature to study the joint beamforming optimization for the wireless powered multi-relay networks considering the imperfect CSI and the practical non-linear EH model. This motivated our work.

In this paper, we study a wireless powered multi-relay multi-user network, in which a multi-antenna base station (BS) wirelessly powers the relays before the information transmission. In addition, we consider the imperfect CSI and non-linear EH model. We aim to minimize the total transmit power at the BS by jointly optimizing the source and relay beamforming weights with the signal-to-noise ratio (SNR) constraints at the users and the energy causality constraints at the relays. The formulated optimization problem is non-convex, and thus, it is difficult to solve. To tackle this, we first transform the non-convex problem into a worst-case optimization, and then, we develop an iterative algorithm based on alternating optimization to solve this worst-case optimization. Note that the optimization problem and the proposed algorithms including the transformation and approximation schemes are quite different from any existing works. The simulations results demonstrate the advantage of the proposed robust scheme.

Notation: $\mathbf{e}_m$ denotes a vector with its m-th entry equal to one and zero otherwise. $\mathbf{X} \succeq 0$ means that $\mathbf{X}$ is positive-semidefinite. $\mathbf{x} \sim \mathcal{CN}(0, \sigma^2\mathbf{I}_m)$ denotes that $\mathbf{x}$ is a complex Gaussian random vector with mean 0 and covariance matrix $\sigma^2\mathbf{I}_m$. Finally, $\mathcal{N}_m \triangleq \{1, 2, ...m\}$.

II. System Model and Problem Statement

A. System Model

We consider a wireless powered downlink multi-relay multi-user network, where an L-antenna BS transmits information to K single-antenna users as shown in Fig. 1. Due to the absence of the direct channels from the BS to the users, the M half-duplex amplify-and-forward (AF) single-antenna relays assist the transmission. The m-th relay and the k-th user will be denoted by R_m and U_k, respectively, where $m \in \mathcal{N}_M$ and $k \in \mathcal{N}_K$. It is assumed that the relays are energy-constrained, and thus, need to replenish energy from the BS. We also consider the block fading channel: the channel coefficients remain constant in one transmission block of length T and change independently over different blocks. A transmission block is divided into two phases: the EH phase and the information transfer phase. Similar to the related works in the literature [8], [9], [14], it is assumed that perfect synchronization has been established among all nodes prior to the EH and information transmission.

Manuscript received October 19, 2018; revised December 26, 2018; accepted January 26, 2019. Date of publication January 30, 2019; date of current version March 14, 2019. This work was supported in part by the China Scholarship Council (CSC) and in part by NSERC. The review of this paper was coordinated by Prof. S. De. *(Corresponding author: Il-Min Kim.)*

X. Jia and C. Zhang are with the College of Information and Communication Engineering, Harbin Engineering University, Harbin 150001, China (e-mail: jiaxinghuaheu@gmail.com; zhangchaozhu@hrbeu.edu.cn).

I.-M. Kim is with the Department of Electrical and Computer Engineering, Queen's University, Kingston, ON K7L 3N6, Canada (e-mail: ilmin.kim@queensu.ca).

Digital Object Identifier 10.1109/TVT.2019.2896214

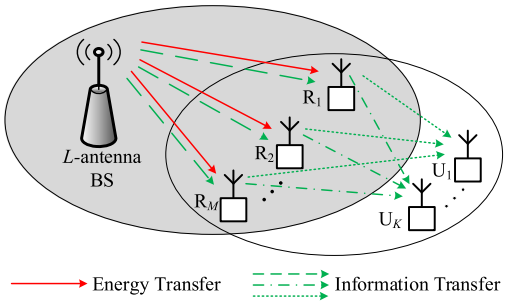

Fig. 1. A wireless powered multirelay multiuser network consisting of an L-antenna base station, M single-antenna relays, and K single-antenna users.

In the EH phase, the BS broadcasts the energy-carrying signals in order to power the relays for the time τT. Let $x_s, \mathbf{z}_s \in \mathbb{C}^L$, and $\mathbf{h}_m \in \mathbb{C}^L$ denote the s-th energy-carrying signal, the energy beamforming vector associated with x_s, and the energy transfer channel vector from the BS to R_m, respectively, where $s \in \mathcal{N}_S$ and $S \leq L$. Also, for any $s \neq s'$, it is assumed that $\mathbb{E}[|x_s|^2] = 1$, $\mathbb{E}[x_s x_{s'}^*] = 0$. Then the signal received at R_m is given by $y_{\mathrm{E},m} = \sum_{s\in\mathcal{N}_S} \mathbf{h}_m^T \mathbf{z}_s x_s + n_{\mathrm{E},m}$, where $n_{\mathrm{E},m} \sim \mathcal{CN}(0, \sigma_{\mathrm{R},m}^2)$ is the additive Gaussian noise. Considering the non-linear EH model as stated in [12], the energy harvested at R_m is given by $Q_{\mathrm{E},m}(\mathbf{Z}) = \frac{\tau T P_s \left[\Theta_m(\mathbf{Z}) - \Omega\right]}{(1-\Omega)}$, where $\Omega \triangleq (1+\mathrm{e}^{AB})^{-1}$ is a constant which ensures a zero-input zero-output response for EH and $\Theta_m(\mathbf{Z}) \triangleq (1+\mathrm{e}^{-A(\mathrm{tr}(\mathbf{h}_m^* \mathbf{h}_m^T \mathbf{Z}) - B)})^{-1}$ is the logistic function. Herein, P_s is the maximum harvested power level at each relay when the EH circuit is saturated. Parameters A and B are positive constants related to the circuit specification. Also, $\mathbf{Z} \triangleq \sum_{s\in\mathcal{N}_S} \mathbf{z}_s \mathbf{z}_s^H$.

In the information transmission phase, the information transmission is completed over K equal-length sub-phases. For any $k \in \mathcal{N}_K$, the k-th sub-phase is partitioned into two equal-length time-slots. In the first time-slot, the BS transmits the information signals $x_{\mathrm{I},k}$ to U_k for the time $\frac{(1-\tau)T}{2K}$, where $\mathbb{E}[|x_{\mathrm{I},k}|^2] = 1$. Then the signal vector received at the relays is given by $\mathbf{y}_{\mathrm{R},k} = \mathbf{F}^T \mathbf{v}_k x_{\mathrm{I},k} + \mathbf{n}_{\mathrm{R}}$, where $\mathbf{v}_k \in \mathbb{C}^L$, $\mathbf{F} \in \mathbb{C}^{L\times M}$, and $\mathbf{n}_{\mathrm{R}} \in \mathbb{C}^M$ denote the beamforming vector associated with $x_{\mathrm{I},k}$, the information channel matrix from the BS to the relays, and the additive Gaussian noise vector with $\mathbf{n}_{\mathrm{R}} \sim \mathcal{CN}(0, \sigma_{\mathrm{R}}^2 \mathbf{I}_M)$, respectively. In the second time-slot, R_m multiplies the received signal by a complex weight $w_{m,k}^*$ and transmits the obtained signal to U_k for the time $\frac{(1-\tau)T}{2K}$. Letting $\mathbf{w}_k \triangleq [w_{1,k}, w_{2,k}, ..., w_{M,k}]^T$ and $\mathbf{W}_k \triangleq \mathrm{diag}(\mathbf{w}_k)$, the relaying power at R_m is given by $P_{m,k}^{\mathrm{R}}(\mathbf{v}_k, \mathbf{w}_k) = \left|\mathbf{e}_m^T \mathbf{W}_k^H \mathbf{F}^T \mathbf{v}_k\right|^2 + \sigma_{\mathrm{R}}^2 \left\|\mathbf{e}_m^T \mathbf{W}_k^H\right\|^2$. The signal received at U_k is given by $y_{\mathrm{U},k} = \mathbf{g}_k^T \mathbf{W}_k^H \mathbf{F}^T \mathbf{v}_k x_{\mathrm{I},k} + \mathbf{g}_k^T \mathbf{W}_k^H \mathbf{n}_{\mathrm{R}} + n_k$, where $\mathbf{g}_k \in \mathbb{C}^M$ and $n_k \sim \mathcal{CN}(0, \sigma_{\mathrm{U},k}^2)$ denote the information channel vector from the relays to U_k and the additive Gaussian noise at U_k, respectively. The SNR from the BS to U_k is given by $\Gamma_k(\mathbf{v}_k, \mathbf{w}_k) = \frac{\left|\mathbf{g}_k^T \mathbf{W}_k^H \mathbf{F}^T \mathbf{v}_k\right|^2}{\sigma_{\mathrm{R}}^2 \left\|\mathbf{g}_k^T \mathbf{W}_k^H\right\|^2 + \sigma_{\mathrm{U},k}^2}$.

In this paper, we use the channel model with imperfect CSI, which has been widely adopted in the literature including [14]. Letting $\mathbf{F} \triangleq [\mathbf{f}_1, \mathbf{f}_2, ..., \mathbf{f}_M]$ and $\mathbf{g}_k \triangleq [g_{k,1}, g_{k,2}, ..., g_{k,M}]^T$, the norm-bounded imperfect channels are modeled as $\mathbf{h}_m \triangleq \hat{\mathbf{h}}_m + \Delta_{\mathbf{h}_m}, \forall m$, $\mathbf{f}_m \triangleq \hat{\mathbf{f}}_m + \Delta_{\mathbf{f}_m}, \forall m$, and $g_{k,m} \triangleq \hat{g}_{k,m} + \Delta_{g_{k,m}}, \forall m, k$, where $\hat{\mathbf{h}}_m$, $\hat{\mathbf{f}}_m$, and $\hat{g}_{k,m}$ denote the estimated CSI and they are known at the BS. Also, $\Delta_{\mathbf{h}_m}$, $\Delta_{\mathbf{f}_m}$, and $\Delta_{g_{k,m}}$ denote the uncertainties of the corresponding channels, which are assumed to be norm bounded as $\mathcal{H}_1 \triangleq \left\{\{\Delta_{\mathbf{h}_m}\} \middle| \|\Delta_{\mathbf{h}_m}\| \leq \epsilon_{1,m}, \forall m\right\}$, $\mathcal{H}_2 \triangleq \left\{\{\Delta_{\mathbf{f}_m}\} \middle| \|\Delta_{\mathbf{f}_m}\| \leq \epsilon_{2,m}, \forall m\right\}$, and $\mathcal{H}_3 \triangleq \left\{\{\Delta_{g_{k,m}}\} \middle| \|\Delta_{g_{k,m}}\| \leq \epsilon_{3,m}, \forall m, k\right\}$. We assume that all the optimization calculation and coordination are operated at the BS, and then, one can execute the coordination mechanism stated in [8]. During the coordination above, the base station (i.e., the coordinator) has to send the control signals to all other nodes, i.e., the relays and the users, to ensure the perfect coordination. Note that we assume imperfect CSI at the BS and users considering that only (very) limited power can be used by the EH relays for pilot transmissions, which is in sharp contrast to the existing works that assuming perfect CSI [4]–[6], [8], [9]. Also, it is worth to note that, following the coordination mechanism above, the relays do not need any CSI for themselves because the relays operate with the AF scheme.

The proposed network can be applied to many communications scenarios such as the wireless sensor networks, the device-to-device (D2D) networks, and the IoT networks. Due to the severe pathless (e.g., from the rough terrain, the building obstacles, etc.), it is assumed that the communication source has no direct channels to the destinations nodes, and thus, the EH relays are deployed to assist the transmission.

B. Problem Statement

We aim to minimize the total transmit power at the BS by jointly optimizing the energy beamforming matrix $\mathbf{Z}$, the source beamforming vectors $\{\mathbf{v}_k\}$, and the relaying beamforming vectors $\{\mathbf{w}_k\}$. Overall, the optimization problem is given by

$$\min_{\mathbf{Z}\succeq\mathbf{0}, \{\mathbf{w}_k\}, \{\mathbf{v}_k\}} \mathrm{tr}(\mathbf{Z}) + \sum_{k\in\mathcal{N}_K} \|\mathbf{v}_k\|^2 \tag{1a}$$

$$\text{s.t.} \min_{\substack{\{\Delta_{\mathbf{g}_k}\}\in\mathcal{H}_3,\\ \Delta_{\mathbf{F}}\in\mathcal{H}_2}} \frac{\left|(\hat{\mathbf{g}}_k + \Delta_{\mathbf{g}_k})^T \mathbf{W}_k^H (\hat{\mathbf{F}} + \Delta_{\mathbf{F}})^T \mathbf{v}_k\right|^2}{\sigma_{\mathrm{R}}^2 \left\|(\hat{\mathbf{g}}_k + \Delta_{\mathbf{g}_k})^T \mathbf{W}_k^H\right\|^2 + \sigma_{\mathrm{U},k}^2} \geq \gamma_k, \forall k, \tag{1b}$$

$$\max_{\Delta_{\mathbf{F}}\in\mathcal{H}_2} \sum_{k\in\mathcal{N}_K} \left(|\mathbf{e}_m^T \mathbf{W}_k^H (\hat{\mathbf{F}} + \Delta_{\mathbf{F}})^T \mathbf{v}_k|^2 + \sigma_{\mathrm{R}}^2 \|\mathbf{e}_m^T \mathbf{W}_k^H\|^2\right) \frac{1-\tau}{2K}$$

$$\leq \min_{\{\Delta_{\mathbf{h}_m}\}\in\mathcal{H}_1} \frac{\tau P_s \left[\left(1+\mathrm{e}^{-A\left(\mathrm{tr}\left(\mathbf{H}_m(\Delta_{\mathbf{h}_m})\mathbf{Z}\right)-B\right)}\right)^{-1} - \Omega\right]}{1-\Omega}, \forall m, \tag{1c}$$

where $\hat{\mathbf{g}}_k \triangleq [\hat{g}_{k,1}, \hat{g}_{k,2}, ..., \hat{g}_{k,M}]^T$, $\hat{\mathbf{F}} \triangleq [\hat{\mathbf{f}}_1, \hat{\mathbf{f}}_2, ..., \hat{\mathbf{f}}_M]$, $\Delta_{\mathbf{g}_k} \triangleq [\Delta_{g_{k,1}}, \Delta_{g_{k,2}}, ..., \Delta_{g_{k,M}}]^T$, $\Delta_{\mathbf{F}} \triangleq [\Delta_{\mathbf{f}_1}, \Delta_{\mathbf{f}_2}, ..., \Delta_{\mathbf{f}_M}]$, $\mathbf{H}_m(\Delta_{\mathbf{h}_m}) \triangleq (\hat{\mathbf{h}}_m + \Delta_{\mathbf{h}_m})^*(\hat{\mathbf{h}}_m + \Delta_{\mathbf{h}_m})^T$, and γ_k denotes the given threshold for the SNR at U_k. In the problem (1), (1b) represents that the SNR at U_k must be no smaller than the given threshold γ_k. (1c) is the energy causality constraint at each relay: it means that the energy consumed for relaying must be no greater than the energy harvested at each relay. Due to the couplings among the design variables and the CSI uncertainty, the problem (1) is highly non-convex, and thus, it is difficult to solve. In the next section, we tackle the problem (1).

III. Robust Beamforming

In this section, we first tackle the CSI uncertainty by transforming the problem (1) into a worst-case optimization i.e., robust beamforming optimization. Then, we solve this robust optimization by developing an iterative algorithm based on the alternating optimization.

A. Worst-Case Optimization Transformation

Clearly, the problem (1) is very challenging to solve because there exist additional maximizations and minimizations over $\Delta_{\mathbf{g}_k}$, $\Delta_{\mathbf{F}}$, and $\Delta_{\mathbf{h}_m}$ in the constraints. In the following, we tackle these additional maximizations and minimizations.

Letting $\tilde{\mathbf{W}}_k \triangleq [w_{1,k}\mathbf{I}_L, w_{2,k}\mathbf{I}_L, \ldots, w_{M,k}\mathbf{I}_L]$, we have

$$\begin{aligned}&\left|(\hat{\mathbf{g}}_k + \Delta_{\mathbf{g}_k})^T \mathbf{W}_k^H (\hat{\mathbf{F}} + \Delta_{\mathbf{F}})^T \mathbf{v}_k\right|^2 \\ &= \mathbf{v}_k^H \tilde{\mathbf{W}}_k (\hat{\mathbf{\Psi}}_k + \Delta_{\mathbf{\Psi}_k}) \tilde{\mathbf{W}}_k^H \mathbf{v}_k, \end{aligned} \tag{2}$$

where $\hat{\mathbf{\Psi}}_k \triangleq \hat{\boldsymbol{\psi}}_k^* \hat{\boldsymbol{\psi}}_k^T$, $\Delta_{\mathbf{\Psi}_k} \triangleq \hat{\boldsymbol{\psi}}_k^* \Delta_{\boldsymbol{\psi}_k}^T + \Delta_{\boldsymbol{\psi}_k}^* \hat{\boldsymbol{\psi}}_k^T + \Delta_{\boldsymbol{\psi}_k}^* \Delta_{\boldsymbol{\psi}_k}^T$, $\hat{\boldsymbol{\psi}}_k \triangleq [\hat{g}_{k,1}\hat{\mathbf{f}}_1^T, \hat{g}_{k,2}\hat{\mathbf{f}}_2^T, \ldots, \hat{g}_{k,M}\hat{\mathbf{f}}_M^T]^T$, $\Delta_{\boldsymbol{\psi}_k} \triangleq [\mathbf{b}_{k,1}^T, \mathbf{b}_{k,2}^T, \ldots, \mathbf{b}_{k,M}^T]^T$, and $\mathbf{b}_{k,m} \triangleq \Delta_{g_{k,m}} \hat{\mathbf{f}}_m + \hat{g}_{k,m} \Delta_{\mathbf{f}_m} + \Delta_{g_{k,m}} \Delta_{\mathbf{f}_m}$. In addition, one can obtain

$$\begin{aligned}\|\Delta_{\boldsymbol{\psi}_k}\|^2 &\le \sum_{m\in\mathcal{N}_M} \left(\|\Delta_{g_{k,m}} \hat{\mathbf{f}}_m\| + \|\hat{g}_{k,m} \Delta_{\mathbf{f}_m}\| + \|\Delta_{g_{k,m}} \Delta_{\mathbf{f}_m}\|\right)^2 \\ &\le \sum_{m\in\mathcal{N}_M} \left(|\Delta_{g_{k,m}}| \|\hat{\mathbf{f}}_m\| + \left(|\hat{g}_{k,m}| + |\Delta_{g_{k,m}}|\right)\|\Delta_{\mathbf{f}_m}\|\right)^2 \\ &\le \sum_{m\in\mathcal{N}_M} \left(\epsilon_{3,m}\|\hat{\mathbf{f}}_m\| + \epsilon_{3,m}\epsilon_{2,m} + \epsilon_{2,m}|\hat{g}_{k,m}|\right)^2, \end{aligned} \tag{3}$$

$$\begin{aligned}\|\Delta_{\mathbf{\Psi}_k}\| &\le \|\hat{\boldsymbol{\psi}}_k^* \Delta_{\boldsymbol{\psi}_k}^T\| + \|\Delta_{\boldsymbol{\psi}_k}^* \hat{\boldsymbol{\psi}}_k^T\| + \|\Delta_{\boldsymbol{\psi}_k}^* \Delta_{\boldsymbol{\psi}_k}^T\| \\ &\le \|\hat{\boldsymbol{\psi}}_k^*\| \|\Delta_{\boldsymbol{\psi}_k}^T\| + \|\Delta_{\boldsymbol{\psi}_k}^*\| \|\hat{\boldsymbol{\psi}}_k^T\| + \|\Delta_{\boldsymbol{\psi}_k}^*\| \|\Delta_{\boldsymbol{\psi}_k}^T\| \\ &\le \epsilon_{4,k}^2 + 2\epsilon_{4,k}\|\hat{\boldsymbol{\psi}}_k\|, \end{aligned} \tag{4}$$

where $\epsilon_{4,k} \triangleq \sqrt{\sum_{m\in\mathcal{N}_M} (\epsilon_{3,m}\|\hat{\mathbf{f}}_m\| + \epsilon_{3,m}\epsilon_{2,m} + \epsilon_{2,m}|\hat{g}_{k,m}|)^2}$. Letting $\Delta_{\mathbf{G}_k} \triangleq \mathrm{diag}(\hat{\mathbf{g}}_k)\mathrm{diag}(\Delta_{\mathbf{g}_k})^H + \mathrm{diag}(\Delta_{\mathbf{g}_k})\mathrm{diag}(\hat{\mathbf{g}}_k)^H + \mathrm{diag}(\Delta_{\mathbf{g}_k})\mathrm{diag}(\Delta_{\mathbf{g}_k})^H$ and $\hat{\mathbf{G}}_k \triangleq \mathrm{diag}(\hat{\mathbf{g}}_k)\mathrm{diag}(\hat{\mathbf{g}}_k)^H$, we have

$$\left\|(\hat{\mathbf{g}}_k + \Delta_{\mathbf{g}_k})^T \mathbf{W}_k^H\right\|^2 = \mathbf{w}_k^H (\hat{\mathbf{G}}_k + \Delta_{\mathbf{G}_k}) \mathbf{w}_k. \tag{5}$$

Herein, we have

$$\begin{aligned}\|\Delta_{\mathbf{G}_k}\| &\le \|\mathrm{diag}(\hat{\mathbf{g}}_k)\mathrm{diag}(\Delta_{\mathbf{g}_k})^H\| + \|\mathrm{diag}(\Delta_{\mathbf{g}_k})\mathrm{diag}(\hat{\mathbf{g}}_k)^H\| \\ &\quad + \|\mathrm{diag}(\Delta_{\mathbf{g}_k})\mathrm{diag}(\Delta_{\mathbf{g}_k})^H\| \\ &\le \|\hat{\mathbf{g}}_k\| \|\Delta_{\mathbf{g}_k}^H\| + \|\Delta_{\mathbf{g}_k}\| \|\hat{\mathbf{g}}_k^H\| + \|\Delta_{\mathbf{g}_k}\| \|\Delta_{\mathbf{g}_k}^H\| \\ &\le \sum_{m\in\mathcal{N}_M} \epsilon_{3,m}^2 + 2\sqrt{\sum\nolimits_{m\in\mathcal{N}_M} \epsilon_{3,m}^2}\,\|\hat{\mathbf{g}}_k\|. \end{aligned} \tag{6}$$

Based on the analysis above, in order to minimize the left-hand side (LHS) of (1b), we obtain its lower bound as follows:

$$\begin{aligned}&\frac{\left|(\hat{\mathbf{g}}_k + \Delta_{\mathbf{g}_k})^T \mathbf{W}_k^H (\hat{\mathbf{F}} + \Delta_{\mathbf{F}})^T \mathbf{v}_k\right|^2}{\sigma_{\mathrm{R}}^2 \left\|(\hat{\mathbf{g}}_k + \Delta_{\mathbf{g}_k})^T \mathbf{W}_k^H\right\|^2 + \sigma_{\mathrm{U},k}^2} \\ &\ge \frac{\mathbf{v}_k^H \tilde{\mathbf{W}}_k (\hat{\mathbf{\Psi}}_k - \xi_{1,k}\mathbf{I}_{LM}) \tilde{\mathbf{W}}_k^H \mathbf{v}_k}{\sigma_{\mathrm{R}}^2 \mathbf{w}_k^H (\hat{\mathbf{G}}_k + \xi_{2,k}\mathbf{I}_{LM}) \mathbf{w}_k + \sigma_{\mathrm{U},k}^2}, \end{aligned} \tag{7}$$

where $\xi_{1,k} \triangleq \epsilon_{4,k}^2 + 2\epsilon_{4,k}\|\hat{\boldsymbol{\psi}}_k\|$ and $\xi_{2,k} \triangleq \sum_{m\in\mathcal{N}_M} \epsilon_{3,m}^2 + 2(\sum_{m\in\mathcal{N}_M} \epsilon_{3,m}^2)^{\frac{1}{2}} \|\hat{\mathbf{g}}_k\|$. Similarly, in order to maximize the LHS of (1c) and minimize the right-hand side (RHS) of the (1c), we obtain the upper bound and lower bound as follows:

$$\begin{aligned}&\sum_{k\in\mathcal{N}_K} \left|\mathbf{e}_m^T \mathbf{W}_k^H (\hat{\mathbf{F}} + \Delta_{\mathbf{F}})^T \mathbf{v}_k\right|^2 \\ &= \sum_{k\in\mathcal{N}_K} \mathbf{v}_k^H \tilde{\mathbf{W}}_k (\hat{\boldsymbol{\phi}}_m^* \hat{\boldsymbol{\phi}}_m^T + \Delta_{\mathbf{\Phi}_m}) \tilde{\mathbf{W}}_k^H \mathbf{v}_k \\ &\le \sum_{k\in\mathcal{N}_K} \mathbf{v}_k^H \tilde{\mathbf{W}}_k (\hat{\boldsymbol{\phi}}_m^* \hat{\boldsymbol{\phi}}_m^T + \xi_{3,m} \tilde{\mathbf{I}}_{LM}^m) \tilde{\mathbf{W}}_k^H \mathbf{v}_k, \end{aligned} \tag{8}$$

$$\begin{aligned}&\tau P_s \left[(1 + \mathrm{e}^{-A(\mathrm{tr}(\mathbf{H}_m(\Delta_{\mathbf{h}_m})\mathbf{Z}) - B)})^{-1} - \Omega\right] \\ &= \tau P_s \left[(1 + \mathrm{e}^{-A(\mathrm{tr}((\hat{\mathbf{h}}_m^* \hat{\mathbf{h}}_m^T + \Delta_{\mathbf{H}_m})\mathbf{Z}) - B)})^{-1} - \Omega\right] \\ &\ge \tau P_s \left[(1 + \mathrm{e}^{-A(\mathrm{tr}((\hat{\mathbf{h}}_m^* \hat{\mathbf{h}}_m^T - \xi_{4,m}\mathbf{I}_L)\mathbf{Z}) - B)})^{-1} - \Omega\right], \end{aligned} \tag{9}$$

where $\hat{\boldsymbol{\phi}}_m \triangleq [\mathbf{0}_{1\times L(m-1)}, \mathbf{f}_m^T, \mathbf{0}_{1\times L(M-m)}]^T$, $\Delta_{\mathbf{\Phi}_m} \triangleq \Delta_{\boldsymbol{\phi}_m}^* \Delta_{\boldsymbol{\phi}_m}^T + \Delta_{\boldsymbol{\phi}_m}^* \hat{\boldsymbol{\phi}}_m^T + \hat{\boldsymbol{\phi}}_m^* \Delta_{\boldsymbol{\phi}_m}^T$, $\Delta_{\boldsymbol{\phi}_m} \triangleq [\mathbf{0}_{1\times L(m-1)}, \Delta_{\mathbf{f}_m}^T, \mathbf{0}_{1\times L(M-m)}]^T$, $\tilde{\mathbf{I}}_{LM}^m \triangleq \mathrm{diag}(\mathbf{0}_{1\times L(m-1)}, \mathbf{1}_{1\times L}, \mathbf{0}_{1\times L(M-m)})$, $\xi_{3,m} \triangleq \epsilon_{2,m}^2 + 2\epsilon_{2,m}\|\hat{\mathbf{f}}_m\|$, $\Delta_{\mathbf{H}_m} \triangleq \hat{\mathbf{h}}_m^* \Delta_{\mathbf{h}_m}^T + \Delta_{\mathbf{h}_m}^* \hat{\mathbf{h}}_m^T + \Delta_{\mathbf{h}_m}^* \Delta_{\mathbf{h}_m}^T$, and $\xi_{4,m} \triangleq \epsilon_{1,m}^2 + 2\epsilon_{1,m}\|\hat{\mathbf{h}}_m\|$. Finally, the worst-case problem is given by

$$\min_{\mathbf{Z}\succeq\mathbf{0}, \{\mathbf{w}_k\}, \{\mathbf{v}_k\}} \mathrm{tr}(\mathbf{Z}) + \sum_{k\in\mathcal{N}_K} \|\mathbf{v}_k\|^2 \tag{10a}$$

$$\text{s.t. } \frac{\mathbf{v}_k^H \tilde{\mathbf{W}}_k \mathbf{B}_{1,k} \tilde{\mathbf{W}}_k^H \mathbf{v}_k}{\sigma_{\mathrm{R}}^2 \mathbf{w}_k^H \mathbf{B}_{2,k} \mathbf{w}_k + \sigma_{\mathrm{U},k}^2} \ge \gamma_k, \forall k, \tag{10b}$$

$$\sum_{k\in\mathcal{N}_K} \left(\mathbf{v}_k^H \tilde{\mathbf{W}}_k \mathbf{B}_{3,m} \tilde{\mathbf{W}}_k^H \mathbf{v}_k + \sigma_{\mathrm{R}}^2 \|\mathbf{e}_m^T \mathbf{W}_k^H\|^2\right) \le \frac{2K\tau P_s \left[\left(1 + \mathrm{e}^{-A(\mathrm{tr}(\mathbf{B}_{4,m}\mathbf{Z}) - B)}\right)^{-1} - \Omega\right]}{(1-\tau)(1-\Omega)}, \forall m, \tag{10c}$$

where $\mathbf{B}_{1,k} \triangleq \hat{\mathbf{\Psi}}_k - \xi_{1,k}\mathbf{I}_{LM}$, $\mathbf{B}_{2,k} \triangleq \hat{\mathbf{G}}_k + \xi_{2,k}\mathbf{I}_M$, $\mathbf{B}_{3,m} \triangleq \hat{\boldsymbol{\phi}}_m^* \hat{\boldsymbol{\phi}}_m^T + \xi_{3,m}\tilde{\mathbf{I}}_{LM}^m$, and $\mathbf{B}_{4,m} \triangleq \hat{\mathbf{h}}_m^* \hat{\mathbf{h}}_m^T - \xi_{4,m}\mathbf{I}_L$. Although the problem (1) has been transformed into the worst-case optimization (10), this new problem is still non-convex, which cannot be solved directly. In the following, we will tackle this worst-case problem utilizing the alternating optimization.

B. Proposed Iterative Algorithm

In this subsection, we tackle the problem (10) by alternatively solving three subproblems: (i) optimizing $\{\mathbf{v}_k\}$ with given $\{\mathbf{w}_k\}$ and $\mathbf{Z}$; (ii) optimizing $\mathbf{Z}$ with given $\{\mathbf{w}_k\}$ and $\{\mathbf{v}_k\}$; (iii) optimizing $\{\mathbf{w}_k\}$ with given $\mathbf{Z}$ and $\{\mathbf{v}_k\}$. At each iteration, we solve these three subproblems separately as in the following.

1) Optimizing $\{\mathbf{v}_k\}$ With Given $\{\mathbf{w}_k\}$ and $\mathbf{Z}$: Fixing $\{\mathbf{w}_k\}$ and $\mathbf{Z}$ and letting $\mathbf{V}_k \triangleq \mathbf{v}_k \mathbf{v}_k^H$, $\forall k$, the problem (10) can be relaxed by

$$\min_{\{\mathbf{V}_k\succeq\mathbf{0}\}} \sum_{k\in\mathcal{N}_K} \mathrm{tr}(\mathbf{V}_k) \tag{11a}$$

$$\text{s.t. } \mathrm{tr}(\mathbf{C}_{1,k}\mathbf{V}_k) - \mathrm{tr}(\mathbf{C}_{2,k}\mathbf{V}_k) \ge \tilde{\sigma}_k^2 \gamma_k, \forall k, \tag{11b}$$

$$\sum_{k\in\mathcal{N}_K} \mathrm{tr}(\mathbf{C}_{3,k,m}\mathbf{V}_k) \le \tilde{Q}_{1,m}, \forall m, \tag{11c}$$

where $\mathbf{C}_{1,k} \triangleq \tilde{\mathbf{W}}_k \hat{\mathbf{\Psi}}_k \tilde{\mathbf{W}}_k^H$, $\mathbf{C}_{2,k} \triangleq \tilde{\mathbf{W}}_k \xi_{1,k} \mathbf{I}_{LM} \tilde{\mathbf{W}}_k^H$, $\tilde{\sigma}_k^2 \triangleq \sigma_{\mathrm{R}}^2 \mathbf{w}_k^H \mathbf{B}_{2,k} \mathbf{w}_k + \sigma_{\mathrm{U},k}^2$, $\mathbf{C}_{3,k,m} \triangleq \tilde{\mathbf{W}}_k \mathbf{B}_{3,m} \tilde{\mathbf{W}}_k^H$, and $\tilde{Q}_{1,m} \triangleq \frac{2K\tau P_s \left[(1 + \mathrm{e}^{-A(\mathrm{tr}(\mathbf{B}_{4,m}\mathbf{Z}) - B)})^{-1} - \Omega\right]}{(1-\tau)(1-\Omega)} - \sum_{k\in\mathcal{N}_K} \sigma_{\mathrm{R}}^2 |w_{m,k}|^2$. It is seen that

the problem (11) is convex, which can be solved by the interior-point method. To check the tightness of the semidefinite relaxation, we have the following lemma.

Lemma 1: The optimal $\mathbf{V}_k$, also denoted by $\mathbf{V}_k^{\mathrm{opt}}$, to (11) is always rank-one for any $k \in \mathcal{N}_K$.

Proof: See Appendix A. ∎

From Lemma 1, one can see that the optimal $\mathbf{v}_k$ can be obtained by the rank-one decomposition of $\mathbf{V}_k^{\mathrm{opt}}, \forall k$.

2) Optimizing $\mathbf{Z}$ With Given $\{\mathbf{w}_k\}$ and $\{\mathbf{v}_k\}$: Fixing $\{\mathbf{w}_k\}$ and $\{\mathbf{v}_k\}$, the problem (10) can be rewritten by

$$\min_{\mathbf{Z}\succeq\mathbf{0}} \mathrm{tr}(\mathbf{Z}) \text{ s.t. } \tilde{Q}_{2,m} \le \mathrm{tr}(\mathbf{B}_{4,m}\mathbf{Z}), \forall m, \tag{12}$$

where $\tilde{Q}_{2,m} \triangleq \frac{-1}{A}\ln\left((\Omega + \frac{(1-\tau)(1-\Omega)}{2K\tau P_s}\iota_m)^{-1} - 1\right) + B$ and $\iota_m \triangleq \sum_{k\in\mathcal{N}_K}\left(\mathbf{v}_k^H\tilde{\mathbf{W}}_k\mathbf{B}_{3,m}\tilde{\mathbf{W}}_k^H\mathbf{v}_k + \sigma_{\mathrm{R}}^2\left\|\mathbf{e}_m^T\mathbf{W}_k^H\right\|^2\right)$. The problem (12) is convex, and can be solved by the interior-point method.

3) Optimizing $\{\mathbf{w}_k\}$ With Given $\mathbf{Z}$ and $\{\mathbf{v}_k\}$: Fixing $\mathbf{Z}$ and $\{\mathbf{v}_k\}$, the problem (10) can be rewritten by

$$\text{find} \quad \{\mathbf{w}_k\} \tag{13a}$$

$$\text{s.t.} \quad \frac{\mathbf{w}_k^H(\mathbf{m}_k\mathbf{m}_k^H - \mathbf{D}_{1,k})\mathbf{w}_k}{\sigma_{\mathrm{R}}^2\mathbf{w}_k^H\mathbf{B}_{2,k}\mathbf{w}_k + \sigma_{\mathrm{U},k}^2} \ge \gamma_k, \forall k, \tag{13b}$$

$$\sum_{k\in\mathcal{N}_K}\mathbf{w}_k^H\mathbf{D}_{2,k,m}\mathbf{w}_k \le \tilde{Q}_{3,m}, \forall m, \tag{13c}$$

where $\mathbf{m}_k \triangleq \tilde{\mathbf{V}}_k\hat{\boldsymbol{\psi}}_k$, $\mathbf{D}_{1,k} \triangleq \tilde{\mathbf{V}}_k\xi_{1,k}\mathbf{I}_{LM}\tilde{\mathbf{V}}_k^H$, $\mathbf{D}_{2,k,m} \triangleq \tilde{\mathbf{V}}_k\mathbf{B}_{3,m}^T\tilde{\mathbf{V}}_k^H + \sigma_{\mathrm{R}}^2\mathrm{diag}(\mathbf{e}_m)$, and $\tilde{Q}_{3,m} \triangleq \frac{2K\tau P_s[(1+\mathrm{e}^{-A(\mathrm{tr}(\mathbf{B}_{4,m}\mathbf{Z})-B)})^{-1}-\Omega]}{(1-\tau)(1-\Omega)}$. Herein, $\tilde{\mathbf{V}}_k \triangleq [\tilde{\mathbf{v}}_{k,1}, \tilde{\mathbf{v}}_{k,2}, ..., \tilde{\mathbf{v}}_{k,M}]^T$ and $\tilde{\mathbf{v}}_{k,m} \triangleq [\mathbf{0}_{1\times L(m-1)}, \mathbf{v}_k^T, \mathbf{0}_{1\times L(M-m)}]^T$. In the problem (13), the matrices $\{\mathbf{D}_{1,k}\}$ and $\{\mathbf{D}_{2,k,m}\}$ can be reformulated as $\mathbf{D}_{1,k} = \xi_{1,k}\|\mathbf{v}_k\|^2\mathbf{I}_M$ and $\mathbf{D}_{2,k,m} = \mathrm{diag}(\mathbf{e}_m)\left(\mathrm{diag}(|\mathbf{v}_k^T\mathbf{f}_1|^2, ..., |\mathbf{v}_k^T\mathbf{f}_M|^2) + (\xi_{3,m}\|\mathbf{v}_k\|^2 + \sigma_{\mathrm{R}}^2)\mathbf{I}_M\right)$, $\forall k, m$. Then, from the transformations above and $\mathbf{B}_{2,k} = \mathrm{diag}(\hat{\mathbf{g}}_k)\mathrm{diag}(\hat{\mathbf{g}}_k)^H + \xi_{2,k}\mathbf{I}_M$, one can observe that $\{\mathbf{D}_{1,k}\}$, $\{\mathbf{D}_{2,k,m}\}$, and $\{\mathbf{B}_{2,k}\}$ are real-value diagonal matrices. It means that the phase-optimality holds for the problem (13) [14]. That is, $\mathfrak{Im}(\mathbf{w}_k^H\mathbf{m}_k) = 0, \forall k$. Thus, the problem (13) can be reformulated as

$$\begin{aligned}&\text{find} \quad \{\mathbf{w}_k\}\\ &\text{s.t. } \mathfrak{Re}\left(\mathbf{w}_k^H\mathbf{m}_k\right) \ge \sqrt{\mathbf{w}_k^H(\mathbf{D}_{1,k} + \gamma_k\sigma_{\mathrm{R}}^2\mathbf{B}_{2,k})\mathbf{w}_k + \gamma_k\sigma_{\mathrm{U},k}^2}, \forall k,\\ &\quad \mathfrak{Im}\left(\mathbf{w}_k^H\mathbf{m}_k\right) = 0, \forall k, (13c).\end{aligned} \tag{14}$$

It can be seen that the problem (14) is convex. However, there might be more than one solution to the problem (14), which will be against the existence and uniqueness (EU) assumption of alternating optimization [15]. In order to find a unique solution to the problem (14), we rewrite the problem (14) by

$$\begin{aligned}&\max_{\{\mathbf{w}_k\},\{t_k\ge 0\}} \quad \sum_{k\in\mathcal{N}_K} t_k\\ &\text{s.t. } \mathfrak{Im}\left(\mathbf{w}_k^H\mathbf{m}_k\right) = 0, \forall k, (13c),\\ &\mathfrak{Re}\left(\mathbf{w}_k^H\mathbf{m}_k\right) \ge t_k + \sqrt{\mathbf{w}_k^H(\mathbf{D}_{1,k} + \gamma_k\sigma_{\mathrm{R}}^2\mathbf{B}_{2,k})\mathbf{w}_k + \gamma_k\sigma_{\mathrm{U},k}^2}, \forall k,\end{aligned} \tag{15}$$

where $\{t_k\}$ are introduced as auxiliary variables. It can be proved that the unique solution to the problem (15) is also optimal to the problem (13). Also, (15) is convex, and can be solved by the interior-point method.

Overall, the proposed iterative algorithm is summarized in Algorithm 1.

Algorithm 1: Proposed Iterative Algorithm to Solve (10).

Initialize feasible $\{\mathbf{v}_k^{(0)}\}$ and $\mathbf{Z}^{(0)}$ for (15), and set $r = 0$.
repeat
  Solve (15) with given $\{\mathbf{v}_k^{(r)}\}$ and $\mathbf{Z}^{(r)}$ to obtain the optimal $\{\mathbf{w}_k\}$, i.e., $\{\mathbf{w}_k^{(r)}\}$.
  Solve (12) with given $\{\mathbf{w}_k^{(r)}\}$ and $\{\mathbf{v}_k^{(r)}\}$ to obtain the optimal $\mathbf{Z}$, i.e., $\mathbf{Z}^{(r+1)}$.
  Solve (11) with given $\{\mathbf{w}_k^{(r)}\}$ and $\{\mathbf{Z}^{(r+1)}\}$ to obtain the optimal $\{\mathbf{V}_k\}$, i.e., $\{\mathbf{V}_k^{\mathrm{opt}}\}$; obtain $\{\mathbf{v}_k^{(r+1)}\}$ according to the rank-one decompositions of $\{\mathbf{V}_k^{\mathrm{opt}}\}$.
  $r := r + 1$.
until convergence.

4) Convergence and Complexity Analysis: From the descriptions of Algorithm 1, it is easy to see that each subproblem can always achieve a unique solution. i.e. the EU assumption holds. Then according to [15], one can prove that the power sequence comprised of the total transmit power obtained at each iteration is monotonically decreasing and lower-bounded, and thus, the convergence of Algorithm 1 is ensured. The problems (11) and (12) are both the linear semidefinite programming, and the computational complexities are, respectively, given by $\mathfrak{C}_{(11)} = \mathcal{O}((M+K)^{0.5}(L^2(2K+M)+K^2+M^2))$ and $\mathfrak{C}_{(12)} = \mathcal{O}(L^2(M^{1.5}+M^{0.5})+M^{2.5})$ [16]. In the problem (15), one can observe that the optimal phase of $\mathbf{w}_k$ is equivalent to that of $\mathbf{m}_k, \forall k$. Then (15) can be converted into a real-value second-order cone programming, and the computational complexity is given by $\mathfrak{C}_{(15)} = \mathcal{O}((M+K)^{0.5}K^3M(M+1)^3)$. Overall, the computational complexity of Algorithm 1 is given by $\mathfrak{C}_{\mathrm{s}} = I_{\mathrm{it}}(\mathfrak{C}_{(11)} + \mathfrak{C}_{(12)} + \mathfrak{C}_{(15)})$, where I_{it} denotes the iteration number for the convergence.

IV. Numerical Results

In this section, the numerical results are presented to evaluate the performance of the proposed robust scheme. We consider the Rayleigh-fading channels with the path loss of $D^{-\chi}$, where D and χ denote the distance between two transceivers and the path-loss exponent, respectively. It is assumed that the distances between the BS and the relays and between the users and the relays are equal to $D_0 = 12$ m. The channel gains are given by $\mathbf{F} = D_0^{-\frac{\chi}{2}}\tilde{\mathbf{F}}$, $\mathbf{g}_k = D_0^{-\frac{\chi}{2}}\tilde{\mathbf{g}}_k$, and $\mathbf{h}_m = D_0^{-\frac{\chi}{2}}\tilde{\mathbf{h}}_m$, where all the entries of $\tilde{\mathbf{F}}, \tilde{\mathbf{g}}_k$, and $\tilde{\mathbf{h}}_m$ are generated as the Gaussian random variables with zero mean and unit variance. Throughout all simulations, we set $\epsilon_{1,m} = \epsilon_{2,m} = \epsilon_{3,m} = D_0^{-\frac{\chi}{2}}\epsilon_0$, $\gamma_k = 10$ dB, $\chi = 4$, $P_s = 10$ mW, $A = 500$, $B = 0.008$, $\tau = \frac{1}{3}$, $M = K = 5$, and $L = 10$. Unless stated otherwise, ϵ_0 is set to 0.02.

In Fig. 2(a), we present the total transmit power obtained by the proposed algorithm versus iterations for different values of the noise power $\sigma_{\mathrm{R}}^2 = \sigma_{\mathrm{U},k}^2 = \sigma^2$. It can be observed that the proposed algorithm converges very quickly, and obtains the solutions (e.g., within 7 iterations for various values of the noise power). In Fig. 2(b), we present the outage probability of the system versus the channel error ϵ_0. The outage occurs if the SNR constraints or the energy causality constraints are not satisfied. In addition, N denotes the number of the users satisfying the SNR constraints while all the energy causality constraints are satisfied. It can be seen that when the channel error ϵ_0 approaches 0.01, the outage probability of the system with non-robust schemes approaches 1. It means that when ϵ_0 approaches 0.01, the non-robust scheme shows much worst performance, and thus, robust schemes must be considered for this case. In Fig. 2(c), we present the total transmit power obtained by the proposed robust scheme and the non-robust scheme

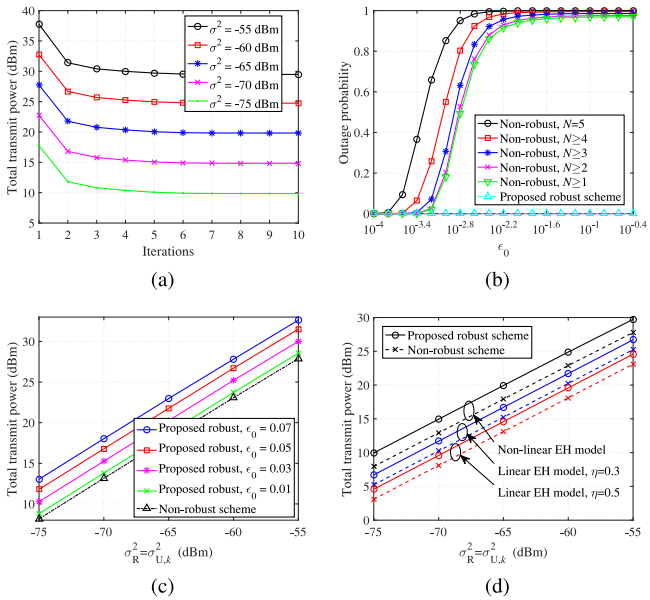

Fig. 2. (a) Total transmit power obtained by the proposed algorithm versus iterations for different $\sigma_{\mathrm{R}}^2 = \sigma_{\mathrm{U},k}^2 = \sigma^2$. (b) Outage probability of the system versus ϵ_0. (c) Total transmit power obtained by the proposed algorithm and the nonrobust scheme versus the noise power $\sigma_{\mathrm{R}}^2 = \sigma_{\mathrm{U},k}^2$ for different ϵ_0. (d) Total transmit power obtained by the proposed robust and nonrobust schemes versus the noise power $\sigma_{\mathrm{R}}^2 = \sigma_{\mathrm{U},k}^2$ with the nonlinear and linear EH models.

versus the noise power $\sigma_{\mathrm{R}}^2 = \sigma_{\mathrm{U},k}^2$ for $\epsilon_0 = \{0.01, 0.03, 0.05, 0.07\}$. It can be seen that the proposed robust scheme requires higher total transmit power compared to the non-robust scheme. Also, when the channel error ϵ_0 increases, the total transmit power increases significantly for various values of the noise power. In Fig. 2(d), we present the total transmit power obtained by the proposed robust and non-robust schemes versus the noise power $\sigma_{\mathrm{R}}^2 = \sigma_{\mathrm{U},k}^2$ with the nonlinear and linear EH models. Herein, we use η to denote the energy conversion efficiency for the linear EH model. It can be seen that the system with non-linear EH model clearly requires higher total transmit power compared to the system with linear EH model. Also, it can be observed that the gap between the total transmit power obtained by the proposed robust scheme and by the non-robust scheme in the system with non-linear EH model is larger than that in the system with linear EH model. This means that the nonlinear EH model is more sensitive to the channel uncertainty compared to the linear EH model in our system.

V. Conclusion

This paper studied joint source and relay beamforming for the wireless powered downlink relaying network, where the non-linear EH model and the imperfect CSI were considered. Our goal was to minimize the total transmit power at the BS by jointly optimizing source beamforming and relay beamforming weights under the energy causality constraints at the relays and the SNR constraints at the users. To solve the formulated problem, we first transformed it into the worst-case optimization, and then, we developed an iterative algorithm to solve this worst-case optimization. Numerical results demonstrated the advantage of the proposed robust scheme.

Appendix A

It is easy to obtain from (11) that $\mathbf{C}_{1,k} \succeq \mathbf{0}$, $\mathbf{C}_{2,k} \succeq \mathbf{0}$, and $\mathbf{C}_{3,k,m} \succeq \mathbf{0}$. Also, $\mathbf{C}_{1,k}$, $\mathbf{C}_{2,k}$, and $\mathbf{C}_{3,k,m}$ can be, respectively, reformulated by $\mathbf{C}_{1,k} = \tilde{\mathbf{W}}_k \hat{\boldsymbol{\psi}}_k^* \hat{\boldsymbol{\psi}}_k^T \tilde{\mathbf{W}}_k^H$, $\mathbf{C}_{2,k} = \xi_{1,k} \|\mathbf{w}_k\|^2 \mathbf{I}_L$, and $\mathbf{C}_{3,k,m} = |w_{m,k}|^2 (\mathbf{f}_m^* \mathbf{f}_m^T + \xi_{3,m} \mathbf{I}_L)$. It follows that $\mathrm{rank}(\mathbf{C}_{1,k}) = 1$ and $\mathrm{rank}(\mathbf{C}_{2,k}) = \mathrm{rank}(\mathbf{C}_{3,k,m}) = L$. Then one can prove that the optimal $\{\mathbf{V}_k\}$ to (11) are always rank-one according to the proof of Proposition 1 in [17].

References

[1] D. Niyato, D.-I. Kim, M. Maso, and Z. Han, "Wireless powered communication networks: Research directions and technological approaches," *IEEE Wireless Commun.*, vol. 24, no. 6, pp. 88–97, Dec. 2017.

[2] B. Clerckx, R. Zhang, R. Schober, D. W. K. Ng, D.-I. Kim, and H. V. Poor, "Fundamentals of wireless information and power transfer: From RF energy harvester models to signal and system designs," *IEEE J. Sel. Areas Commun.*, vol. 37, no. 1, pp. 4–33, Jan. 2019.

[3] H. Tran and G. Kaddoum, "RF wireless power transfer: Regreening future networks," *IEEE Potentials*, vol. 37, no. 2, pp. 35–41, Mar. 2018.

[4] Y. Luo, J. Zhang, and K. B. Letaief, "Transmit power minimization for wireless networks with energy harvesting relays," *IEEE Trans. Commun.*, vol. 64, no. 3, pp. 987–1000, Mar. 2016.

[5] A. A. Nasir, D. T. Ngo, X. Zhou, R. A. Kennedy, and S. Durrani, "Joint resource optimization for multicell networks with wireless energy harvesting relays," *IEEE Trans. Veh. Technol.*, vol. 65, no. 8, pp. 6168–6183, Aug. 2016.

[6] S. Gong, L. Duan, and N. Gautam, "Optimal scheduling and beamforming in relay networks with energy harvesting constraints," *IEEE Trans. Wireless Commun.*, vol. 15, no. 2, pp. 1226–1238, Feb. 2016.

[7] T. Le, G. Kaddoum, and O. Shin, "Joint channel resources allocation and beamforming in energy harvesting systems," *IEEE Wireless Commun. Lett.*, vol. 7, no. 5, pp. 884–887, Oct. 2018.

[8] X. Jia, C. Zhang, J.-M. Kang, and I.-M. Kim, "Joint beamforming design and time allocation for wireless powered asymmetric two-way multirelay network," *IEEE Trans. Veh. Technol.*, vol. 67, no. 10, pp. 9641–9655, Oct. 2018.

[9] S. Salari, I.-M. Kim, D.-I. Kim, and F. Chan, "Joint EH time allocation and distributed beamforming in interference-limited two-way networks with EH-based relays," *IEEE Trans. Wireless Commun.*, vol. 16, no. 10, pp. 6395–6408, Oct. 2017.

[10] B. Clerckx, E. Bayguzina, D. Yates, and P. D. Mitcheson, "Waveform optimization for wireless power transfer with nonlinear energy harvester modeling," in *Proc. Int. Symp. Wireless Commun. Syst.*, Aug. 2015, pp. 276–280.

[11] H. Tran, G. Kaddoum, and K. T. Truong, "Resource allocation in SWIPT networks under a nonlinear energy harvesting model: Power efficiency, user fairness, and channel nonreciprocity," *IEEE Trans. Veh. Technol.*, vol. 67, no. 9, pp. 8466–8480, Sep. 2018.

[12] E. Boshkovska, D. W. K. Ng, N. Zlatanov, and R. Schober, "Practical non-linear energy harvesting model and resource allocation for SWIPT systems," *IEEE Commun. Lett.*, vol. 19, no. 12, pp. 2082–2085, Dec. 2015.

[13] J.-M. Kang, I.-M. Kim, and D.-I. Kim, "Mode switching for SWIPT over fading channel with nonlinear energy harvesting," *IEEE Wireless Commun. Lett.*, vol. 6, no. 5, pp. 678–681, Oct. 2017.

[14] S. Salari, M. Z. Amirani, I.-M. Kim, D.-I. Kim, and J. Yang, "Distributed beamforming in two-way relay networks with interference and imperfect CSI," *IEEE Trans. Wireless Commun.*, vol. 15, no. 6, pp. 4455–4469, Jun. 2016.

[15] J. C. Bezdek and R. J. Hathaway, "Convergence of alternating optimization," *Neural Parallel Sci. Comput.*, vol. 11, no. 4, pp. 351–368, Dec. 2003.

[16] X. Xue, Y. Wang, X. Wang, and T. E. Bogale, "Joint source and relay precoding in multiantenna millimeter-wave systems," *IEEE Trans. Veh. Technol.*, vol. 66, no. 6, pp. 4924–4937, Jun. 2017.

[17] Q. Li, Q. Zhang, and J. Qin, "A special class of fractional QCQP and its applications on cognitive collaborative beamforming," *IEEE Trans. Signal Process.*, vol. 62, no. 8, pp. 2151–2164, Apr. 2014.